

The BAT AGN Spectroscopic Survey – XVIII. Searching for Supermassive Black Hole Binaries in the X-rays

TINGTING LIU,<sup>1</sup> MICHAEL KOSS,<sup>2</sup> LAURA BLECHA,<sup>3</sup> CLAUDIO RICCI,<sup>4,5</sup> BENNY TRAKHTENBROT,<sup>6</sup> RICHARD MUSHOTZKY,<sup>7</sup>  
FIONA HARRISON,<sup>8</sup> KOHEI ICHIKAWA,<sup>9</sup> DARSHAN KAKKAD,<sup>10</sup> KYUSEOK OH,<sup>11,12</sup> MEREDITH POWELL,<sup>13</sup>  
GEORGE C. PRIVON,<sup>14</sup> KEVIN SCHAWINSKI,<sup>15</sup> T. TARO SHIMIZU,<sup>16</sup> KRISTA LYNNE SMITH,<sup>17,18</sup> DANIEL STERN,<sup>19</sup>  
EZEQUIEL TREISTER,<sup>20</sup> AND C. MEGAN URRY<sup>13</sup>

<sup>1</sup>*Center for Gravitation, Cosmology and Astrophysics, Department of Physics, University of Wisconsin-Milwaukee, P.O. Box 413, Milwaukee, WI 53201, USA*

<sup>2</sup>*Eureka Scientific, 2452 Delmer Street Suite 100, Oakland, CA 94602-3017, USA*

<sup>3</sup>*Department of Physics, University of Florida, Gainesville, FL, USA*

<sup>4</sup>*Núcleo de Astronomía de la Facultad de Ingeniería, Universidad Diego Portales, Santiago, Chile*

<sup>5</sup>*Kavli Institute for Astronomy and Astrophysics, Peking University, Beijing 100871, China*

<sup>6</sup>*School of Physics and Astronomy, Tel Aviv University, Tel Aviv 69978, Israel*

<sup>7</sup>*Department of Astronomy, University of Maryland, College Park, MD 20742, USA*

<sup>8</sup>*Cahill Center for Astronomy and Astrophysics, California Institute of Technology, Pasadena, CA 91125, USA*

<sup>9</sup>*Frontier Research Institute for Interdisciplinary Sciences, Tohoku University, Sendai 980-8578, Japan*

<sup>10</sup>*European Southern Observatory, Karl-Schwarzschild-Str. 2, 85748, Garching bei München, Germany*

<sup>11</sup>*Department of Astronomy, Kyoto University, Kyoto 606-8502, Japan*

<sup>12</sup>*JSPS Fellow*

<sup>13</sup>*Department of Physics, Yale University, P.O. Box 2018120, New Haven, CT 06520-8120, USA*

<sup>14</sup>*Department of Astronomy, University of Florida, 211 Bryant Space Sciences Center, Gainesville, FL 32611, USA*

<sup>15</sup>*Department of Physics, ETH Zurich, Wolfgang-Pauli-Strasse 27, CH-8093 Zurich, Switzerland*

<sup>16</sup>*Max-Planck-Institut für extraterrestrische Physik, Postfach 1312, 85741, Garching, Germany*

<sup>17</sup>*KIPAC at SLAC, Stanford University, Menlo Park CA 94025, USA*

<sup>18</sup>*Einstein Fellow*

<sup>19</sup>*Jet Propulsion Laboratory, California Institute of Technology, 4800 Oak Grove Drive, MS 169-224, Pasadena, CA 91109, USA*

<sup>20</sup>*Instituto de Astrofísica, Facultad de Física, Pontificia Universidad Católica de Chile, Casilla 306, Santiago 22, Chile*

(Received xx xx xxxx; Revised xx xx xxxx; Accepted xx xx xxxx)

Submitted to ApJ

## ABSTRACT

Theory predicts that a supermassive black hole binary (SMBHB) could be observed as a luminous active galactic nucleus (AGN) that periodically varies on the order of its orbital timescale. In X-rays, periodic variations could be caused by mechanisms including relativistic Doppler boosting and shocks. Here we present the first systematic search for periodic AGNs using 941 hard X-ray light curves (14–195 keV) from the first 105 months of the *Swift* Burst Alert Telescope (BAT) survey (2004–2013). While we do not find evidence for periodic AGNs in *Swift*-BAT, we have investigated the detectability of SMBHBs in the context of the eROSITA survey by adopting prescriptions for AGN X-ray variability and the periodic variability from a population of SMBHBs and assuming weekly and monthly temporal sampling rates. Even under generous assumptions about the binary population in AGNs, the detectable fraction is modest due to the challenge of distinguishing the periodic signal from normal AGN variability. Due to this effect of “red noise”, we instead find that the search for SMBHBs would greatly benefit from sampling a large number of AGNs at lower cadence.

*Keywords:* Active galaxies — Surveys — X-ray sources

arXiv:1912.02837v1 [astro-ph.HE] 5 Dec 2019

Supermassive black hole binaries (SMBHBs) are expected as the result of galaxy mergers (e.g. Begelman et al. 1980), and yet compelling evidence for close-separation SMBHBs has been elusive. Several studies in the past few years have searched for periodically varying quasars as possible SMBHBs in optical time domain surveys, and numerous candidates have been reported (Graham et al. 2015a,b; Charisi et al. 2016; Liu et al. 2015, 2016, 2019). These SMBHB candidates typically have (observed) variability periods of  $\sim$  a few hundred days – thousand days. Assuming circular, Keplerian orbits, their masses ( $\log(M_{\text{BH}}/M_{\odot}) \sim 8 - 10$ ) and periods correspond to binary separations of  $\sim$  centi- to milli-pc, which are several orders of magnitude more compact than the scale that very long baseline interferometry observations are able to resolve currently (e.g. the radio galaxy 0402+379; Rodriguez et al. 2006) or in the future (D’Orazio & Loeb 2018; Burke-Spolaor et al. 2018). These searches for AGN periodicities have been motivated by hydrodynamic and magneto-hydrodynamic simulations which show that accretion onto an SMBHB varies periodically on the order of the binary orbital timescale (e.g. MacFadyen & Milosavljević 2008; Shi et al. 2012; Noble et al. 2012; D’Orazio et al. 2013; Farris et al. 2014; Gold et al. 2014; Bowen et al. 2018, 2019): the torque exerted by the binary opens up a cavity in the disk in which the binary is embedded (“circumbinary disk”), and the gas instead crosses the gap from the inner edge of the circumbinary disk in the form of narrow streams. The gas eventually feeds the individual accretion disks formed around the black holes (“minidisks”) at a rate that is modulated on the binary orbital timescale. Another possible mechanism is when the steady emission from the minidisk is relativistic Doppler boosted for a highly-inclined, close-separation binary system (D’Orazio et al. 2015), which modulates the apparent flux on the binary orbital period. In both mechanisms, periodicities occur for a wide range of mass ratios ( $q$ ) expected from major mergers: hydrodynamic variability is strongest when  $q \gtrsim 0.1$ , as the binary is able to create an overdensity in the inner edge of the circumbinary disk which interacts with the black holes (e.g. Farris et al. 2014). The Doppler boost model favors small mass ratios; however, even in an equal mass binary, periodicity still manifests since the enhancement and the suppression do not cancel.

In the X-ray regime, an SMBHB may also display periodic variability. Similar to the UV/optical, X-ray emissions from the gas bound to the black holes may also experience Doppler boosting (Haiman 2017). Periodicity may also be produced by shocks, when the streams crossing the gap are flung toward by the black holes and

hit the cavity wall of the circumbinary disk twice per orbit (Tang et al. 2018). When the stream joins a minidisk, it shock-heats its outer edge and produces bright X-ray emission at tens – hundreds keV by inverse Compton scattering (Roedig et al. 2014, see also Farris et al. 2015), which is also modulated on the orbital timescale.

Despite these predictions, the X-ray variability signatures of SMBHBs remain largely unexplored. Only recently was an SMBHB candidate reported by Severgnini et al. (2018) in the center of a Seyfert 2 galaxy at  $z = 0.0362$ , MCG+11–11–032. Its light curve<sup>1</sup> from the Burst Alert Telescope (BAT, Barthelmy et al. 2005) onboard the *Neil Gehrels Swift* Observatory (Gehrels et al. 2004) was claimed to show a quasi-periodic variation with a period of about 25 months over the 123-month baseline, suggesting an orbital velocity of the putative SMBHB:  $v \sim 0.06c$ . Interestingly, its X-ray spectrum is best described by an absorbed power law with a reflection component plus two narrow Gaussian components for Fe K $\alpha$ . While the energy of the second component is less well constrained, their separation in energy  $\Delta E$  is consistent with the velocity derived from the variability period, assuming they are produced in either the minidisks or the inner region of the circumbinary disk.

*Swift*-BAT has been observing the hard X-ray sky in the 14–195 keV energy range since its launch. The fifth and the most recent catalog (Oh et al. 2018) includes 105 months of observations from 2004 December to 2013 August and reports 1632 sources, 947 of which are unbeamed active galactic nuclei (AGNs). This is currently the largest sample of hard X-ray selected AGNs with long-temporal-baseline, regular observations, and it presents a unique opportunity to study the hard-X ray variability of AGNs.

Previous AGN variability studies with *Swift*-BAT (Beckmann et al. 2007; Caballero-Garcia et al. 2012; Shimizu & Mushotzky 2013; Soldi et al. 2014) have measured the fractional flux variability, structure function, or power spectral density (PSD) of BAT AGNs and studied the correlation of variability with physical properties such as black hole mass and X-ray and bolometric luminosities, AGN type, or energy bands. However, no study has so far systematically searched for periodic variability that may be indicative of close SMBHBs at sub-pc separations. Such a search would complement previous ones with ground-based, optical time domain surveys in two important aspects. First, abundant gas

<sup>1</sup> The yet-unpublished data independently analyzed by the Palermo BAT team at *Istituto Nazionale di Astrofisica* (e.g. Segreto et al. 2010).

is funneled in during (gas-rich) galaxy mergers and thereby powers the SMBHs as luminous quasars (e.g. Di Matteo et al. 2005; Hopkins et al. 2008), but the SMBHs are likely to be enshrouded by gas and dust, resulting in substantial obscuration in the optical, UV, and even soft X-ray bands (e.g. Ricci et al. 2017a). Very hard X-ray ( $> 10$  keV) photons, on the other hand, have a high penetrating power through the obscuring material with column densities upward of  $10^{24}$   $\text{cm}^{-2}$  (e.g. Ricci et al. 2015; Koss et al. 2016) and can therefore potentially reveal SMBH duals and binaries that are inaccessible in the UV/optical (e.g. Koss et al. 2012; Satyapal et al. 2017; Ricci et al. 2017a; Koss et al. 2018).

Second, while previous numerical simulations of SMBHBs show that the accretion rate from the circumbinary disk onto the minidisks is periodically modulated, it may not directly translate to a periodic photon luminosity due to the buffering effect of the minidisk, when its gas inflow timescale is longer than the modulation timescale (e.g. Farris et al. 2014). However, binary-modulated X-ray emission produced by shocks is immune to this effect due to the short timescale of Compton cooling compared to the orbital timescale (see also discussions in e.g. Shi & Krolik 2016 and Krolik et al. 2019).

The ability of *Swift*-BAT to study the full variable X-ray sky in general and variable AGNs in particular will be unmatched until the extended ROentgen Survey with an Imaging Telescope Array (eROSITA; Merloni et al. 2012). It will be much more sensitive to (unobscured) AGNs, many of which will be visited at a high cadence as a result of its scanning strategy.

This paper has the dual goal of performing the first systematic search for periodic AGNs in the X-rays and investigating the prospects for detecting SMBHBs with *eROSITA* and is organized as follows: in Sections 2, we search for periodic signals in the 105-month BAT catalog by first modeling the underlying normal AGN variability, which is characterized by higher variability power at lower frequencies (“red noise”). We also revisit the binary candidate MCG+11–11–032 reported by Severgnini et al. (2018). In Section 3, we investigate the detectability of periodic variations in red noise by BAT and the upcoming *eROSITA* survey. We present our conclusions in Section 4.

## 2. BAT AGNS

### 2.1. The 105-month *Swift*-BAT Catalog

*Swift*-BAT has a wide field-of-view (FOV  $\sim 60^\circ \times 100^\circ$ ) and is designed to monitor a comparatively large fraction of the sky for gamma-ray bursts (GRBs). While it is scanning the sky for GRBs and other hard X-ray

transients, BAT is also effectively performing a survey of the full sky with a nearly uniform coverage, with 90% of the sky covered at the 11 Ms level over the period of 105 months, and the median  $5\sigma$  sensitivity limit corresponds to  $7.24 \times 10^{-12}$   $\text{erg cm}^{-2} \text{s}^{-1}$  (Oh et al. 2018). By comparison, the *International Gamma-Ray Astrophysics Laboratory* (INTEGRAL; Ubertini et al. 2003) has primarily observed the Galactic plane with its Imager on Board the *INTEGRAL* Satellite (IBIS; Winkler et al. 2003) in the 17 – 100 keV range with shorter overall exposure time (Bird et al. 2010; Krivonos et al. 2010). *NuSTAR* (Harrison et al. 2013) has a superior sensitivity in the hard X-ray band ( $3\sigma$  sensitivity at  $10^{-14}$   $\text{erg cm}^{-2} \text{s}^{-1}$  in the 10–30 keV range), however it has a smaller field of view ( $12'.2 \times 12'.2$ ) and mostly performs pointed observations.

Following the earlier survey catalogs (Markwardt et al. 2005; Tueller et al. 2008, 2010; Baumgartner et al. 2013), the fifth *Swift*-BAT catalog<sup>2</sup> (Oh et al. 2018) contains 1632 sources observed during the 105 months between 2004 December and 2013 August, 328 of which are newly-identified sources since its last version, the 70-month catalog (Baumgartner et al. 2013). After making a blind source detection at the  $4.8\sigma$  level and fitting for the source position, a cross-search using a fixed radius is made in the archive for counterparts observed by other telescopes/instruments such as *Swift*-XRT, *Chandra*, and *XMM-Newton*. The X-ray sources are also searched for optical counterparts in the NED and SIMBAD databases. Sources with known types in their optical counterparts are further divided into classes, and the 105-month catalog includes 947 un-beamed AGNs, i.e. classified as Seyfert 1, Seyfert 2, or LINER based on their emission lines as well as “Unknown AGNs”. A detailed description of the BAT hard X-ray survey data can be found in Oh et al. (2018) and references therein. One of the main data products is the light curves of BAT-detected sources spanning the duration of the survey. Instead of “snapshot” light curves from individual observations, the 105-month catalog presents the monthly-binned light curves, by adding individual snapshot images from each month of the survey and measuring the source flux from the total-band mosaic image.

Follow-up observations and studies of BAT-detected sources are actively being carried out. Among them is the BAT AGN Spectroscopic Survey<sup>3</sup> (BASS; Koss et al. 2017), a large effort to measure optical spec-

<sup>2</sup> <https://swift.gsfc.nasa.gov/results/bs105mon/>

<sup>3</sup> <http://www.bass-survey.com>

tra for this hard X-ray selected, uniquely-unbiased sample of AGNs with complete estimates for black hole mass, accretion rate, and bolometric luminosity using dedicated spectroscopic observations. In addition to optical spectra, BASS also presents careful determination of the X-ray properties of BAT AGNs by combining *Swift*-BAT data with observations from a variety of soft X-ray telescopes (Ricci et al. 2017b). The BASS sample consists of the brightest ( $L_{2-10\text{keV}} \gtrsim 10^{42} \text{ erg s}^{-1}$ ) and the nearest (90% are at  $z < 0.2$ ) AGNs, allowing detailed studies of nearby AGNs while serving as a benchmark for X-ray surveys of a large sample of high-redshift AGNs, such as the upcoming *eROSITA* and the planned spectroscopic follow-up of *eROSITA*-detected AGNs with SDSS-V (Kollmeier et al. 2017) and 4MOST (Merloni et al. 2019).

## 2.2. Variability Analysis

Our parent sample consists of 941 un-beamed AGNs in the 105-month catalog that are classified as ‘Seyfert 1’, ‘Seyfert 2’ or ‘Unknown AGN’. We first calculate the excess variance (Nandra et al. 1997; Edelson et al. 2002; Vaughan et al. 2003) for each light curve, which removes the apparent variation due to measurement errors:  $\sigma_{\text{xs}}^2 = S^2 - \overline{\sigma_{\text{err}}^2}$ , where  $S^2$  is the variance of the light curve, and  $\sigma_{\text{err}}$  is the measurement error. To select intrinsically variable AGNs<sup>4</sup>, we compare their  $\sigma_{\text{xs}}^2$  with those of galaxy clusters, which are constant hard X-ray sources (e.g. Wik et al. 2011). We have inspected the *Swift*-XRT and *XMM-Newton* data of each cluster, in order to exclude those with contamination from variable AGNs in the BAT FOV. We have also used the detailed analysis of BAT clusters by Ajello et al. (2009) and Ajello et al. (2010). This process removed 8/26 clusters. As we show in Figure 1 (upper panel), the distribution of AGNs closely mimics that of clusters at the  $\sigma_{\text{xs}}^2 < 1.5 \times 10^{-7}$  level, indicating possible remaining systematic effects; above this level, the fraction of galaxy clusters declines to zero. Therefore, we use  $\sigma_{\text{xs}}^2 = 1.5 \times 10^{-7}$  as the variability threshold and select 220 AGNs (23% of the sample) for further analysis.

We have also calculated the fractional variability, which is normalized to the average flux of the source:  $f_{\text{var}} = (\sigma_{\text{XS}} / \langle F \rangle) \times 100\%$ . It is similar to the  $S_V$  parameter used by Soldi et al. (2014), where their  $\sigma_Q$  parameter reduces to  $\sigma_{\text{XS}}$  for uniform measurement errors. As we show in Figure 1 (lower panel), most AGNs in this sample are variable at the 30–40% level on the  $\sim$ month

<sup>4</sup> We assume that all AGNs are likely intrinsically variable at some level. Here we will exclude any AGN whose observed variability is largely due to measurement uncertainties.

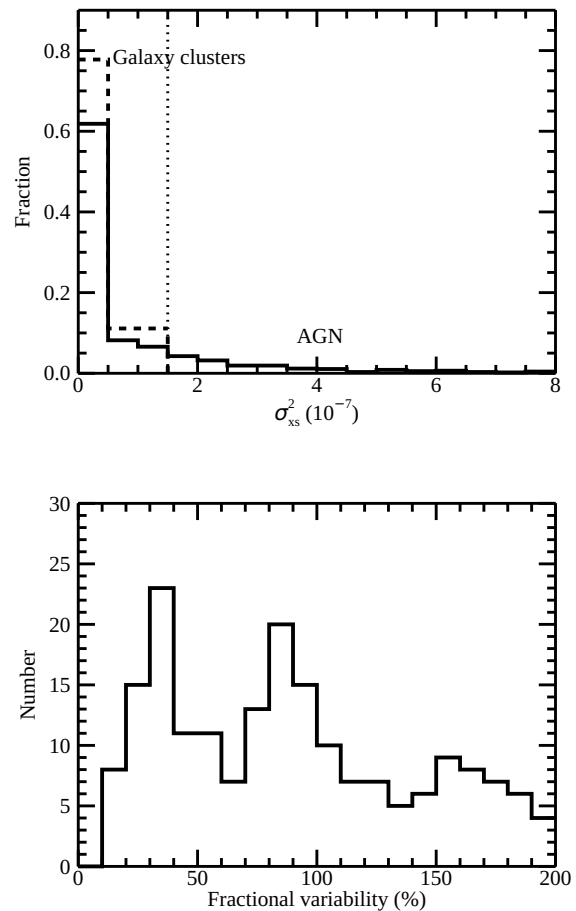


**Figure 1.** Upper panel: the excess variance of the galaxy cluster sample (dashed histogram) versus the full AGN sample (solid histogram). Those with negative excess variance are defined as  $\sigma_{\text{xs}}^2 = 0$ . The variability threshold is marked with a dotted line. Lower panel: the fractional variability distribution of the variable AGN sample. AGNs with fractional variability larger than 200% are defined to have  $f_{\text{var}} = 200\%$  (see text).

timescale, similar to the sample from Soldi et al. (2014), although with a heavy tail for AGNs with fractional variability  $\gtrsim 100\%$ . We find that those high-variance values ( $f_{\text{var}} > 50\%$ ) tend to be associated with low count rates. Additionally, visual inspection of their light curves reveals a number of outliers, and thus we only show  $f_{\text{var}} \leq 200\%$  in Figure 1 for presentation purposes. We confirm that by using  $\sigma_{\text{xs}}^2$  instead of  $f_{\text{var}}$  as the variability threshold, we do not systematically bias against faint sources, as the mode count rates of the selected variable AGNs and those of “non-variable” AGNs are both  $\approx 5 \times 10^{-4} \text{ cts s}^{-1}$

Since the 105-month light curves are uniformly sampled on monthly timescales, we compute the peri-

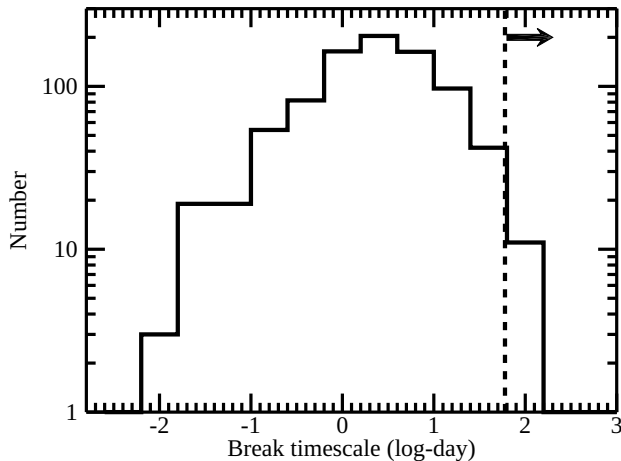


**Figure 2.** The expected PSD break timescales in units of log-day derived from the relation in González-Martín & Vaughan (2012) for the BAT AGNs with black hole mass measurements from BASS DR2. Note that the y-axis is log-scale for clarity. The majority (98%, or 845/861 AGNs) of break timescales are shorter than the variability timescales probed by BAT ( $> 2$  months, to the right of the dashed line).

odogram, which is defined as the modulus squared of the Fourier transform and is normalized to have units of  $(\text{rms}/\text{mean})^2 \text{ Hz}^{-1}$ . We ignore the point at the Nyquist frequency<sup>5</sup> and fit a simple linear function to the periodogram in log-space and estimate the power law continuum of the power spectrum, where here we have corrected for the bias between the periodogram and the power spectrum by adding 0.25068 to the best fit linear function (see Papadakis & Lawrence 1993; Vaughan 2005).

We confirm the goodness-of-fit using the Kuiper’s test, since the periodogram should scatter around the true PSD following a  $\chi^2$  distribution with two degrees of freedom (e.g. Vaughan 2005). By the same token, a possible feature with a power below  $-\ln[1 - (1 - \epsilon)^{1/n}]P(f)$  can be rejected as a spurious peak at the  $(1 - \epsilon)$  level, where  $\epsilon$  is the chosen false alarm probability, and the trial factor  $n$  is the number of frequency points in the range where the periodogram is fitted.

By fitting a simple linear function to the periodogram, we have assumed that the underlying red noise power spectrum is described by a single power law in the frequency range of interest, and here we show that it

<sup>5</sup> Because the periodogram at this frequency is  $\chi^2_1$ -distributed (e.g. Vaughan 2005).

is indeed a reasonable assumption. Since the break timescale of the X-ray power spectrum is found to correlate with black hole mass (McHardy et al. 2006; González-Martín & Vaughan 2012), we can use the best-fit correlation in González-Martín & Vaughan (2012) to estimate the expected break timescale<sup>6</sup>:  $\log(T_{\text{br}}) = 1.09 \log(M_{\text{BH}}) - 1.70$ , where  $T_{\text{br}}$  is in units of days and  $M_{\text{BH}}$  is in units of  $10^6 M_{\odot}$ . We use black hole masses from the internally-released BASS DR2 (which is soon to be publicly available), which has a higher completion percentage for black hole mass measurements ( $\approx 90\%$ ) than the published DR1 (Koss et al. 2017). Assuming this sample is representative of all BAT AGNs, we expect the majority ( $> 98\%$ ) to have break timescales  $T_{\text{br}} < 2$  month, which corresponds to frequencies that are higher than the Nyquist frequency in our BAT data (Figure 2). This is also consistent with the lack of detection of PSD breaks and the lower limit at  $10^{-6}$  Hz reported by Shimizu & Mushotzky (2013).

Shimizu & Mushotzky (2013) also showed that the brightest AGNs do not become white noise-dominated until the  $\sim 5$ -day timescale, and their power spectra can be well described by single power laws over the full frequency range. However, the fainter sources in our sample show evidence of white noise beginning to dominate at a much lower frequency, and thus we should only fit for the power law continuum in the frequency range where red noise dominates in order to estimate its slope. Hence, for each of the 220 AGNs in our variable sample, we will also consider a “power law+constant” model, in addition to a single power law fit (Section 2.4). Ideally, the constant power level should be consistent with the level of Poisson noise estimated from measurement errors:  $P_{\text{N}} = \frac{2\Delta T \sigma_{\text{err}}^2}{\mu^2}$  (Vaughan et al. 2003), where  $\mu$  is the mean count rate and  $\Delta T = 1$  month for the 105-month BAT light curve. (For example, the power spectrum of a constant X-ray source such as a galaxy cluster should be approximately flat and at a level that is consistent with  $P_{\text{N}}$ .)

### 2.3. MCG+11–11–032 Revisited

We first demonstrate this procedure by testing for the reported periodicity in MCG+11–11–032. Since its light curve presented by Severgnini et al. (2018) was independently analyzed by the Palermo team, we retrieved the light curve from their published Third Palermo BAT Catalog (3PBC) instead of the 105-month catalog (Figure 3). We consider the source red-noise dominated,

<sup>6</sup> Here we have assumed there is no significant difference in the PSDs in the soft ( $< 10$  keV) and hard ( $> 10$  keV) X-ray bands (e.g. Shimizu & Mushotzky 2013).

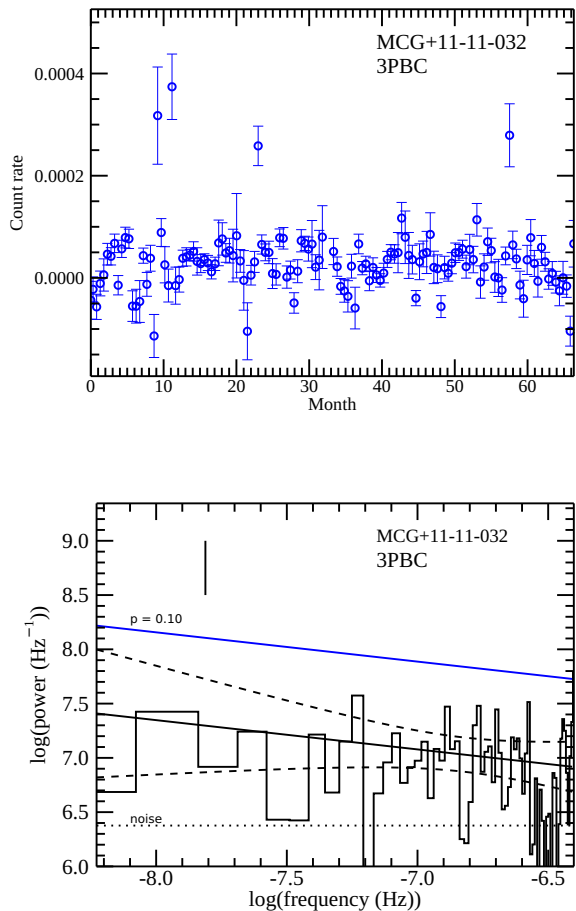


**Figure 3.** Upper panel: the BAT light curve of MCG+11-11-032 since beginning of the mission (Month = 0). The Third Palermo BAT Catalog (3PBC) publishes light curves from the first 66 months of the survey. Lower panel: its power spectrum. Solid line represents the best fit power law continuum, and dashed lines represent model uncertainties, which are determined from the propagation of the uncertainties of the power law slope, normalization, and their covariance (see [Vaughan 2005](#)). The estimated noise level is marked with a dotted line. There is no peak at 25 months (black tick mark) even at the modest 90% level (blue solid line). The four outlying points in the upper panel were not removed in our analysis.

since its power spectrum is significantly above the estimated noise level and the power law slope is not flat after taking into account its uncertainty. Thus, we measure its power spectrum in the full frequency range and are able to reject signals in the full range at the  $> 90\%$  level, including the putative period of 25 months ( $\log[f/\text{Hz}] = -7.8$ ) reported by [Severgnini et al. \(2018\)](#) (Figure 3). However, we note several differences that may result in our different conclusions: [Severgnini et al.](#)

(2018) adopted a different method, where the periodic function is only superimposed for visual purposes, and no systematic search or power spectral analysis was performed. Second, their data were independently processed and were not available to us, so our comparison is not a direct one. Finally, their light curve was from the first 123 months of the survey (which has not been published), and thus robustly detecting two cycles of the signal in the 66-month 3PBC light curve is more difficult.

#### 2.4. The BAT 105-month sample: Power spectrum fitting

We then apply the method to the full sample of 220 variable AGNs in the 105-month dataset. We first naively fit a single power law in the full frequency range and obtain the best-fit power law slope, normalization, and their uncertainties. If the slope is steeper than its uncertainty, then we tentatively classify the power spectrum as “red”, and “white” otherwise. Next, we fit the red power spectra to single power law and power law+constant models using the least squares method and penalize the latter model due to its extra parameter, i.e. the frequency where the power spectrum flattens to a constant. We find that all 220 AGNs can be reasonably described by either a white power spectrum (124/220), or a red single power law power spectrum (96/220).

However, as we previously mentioned, the frequency range where white noise dominates the power spectrum can normally be estimated by comparing the power spectrum with  $P_N$ , in which case a single power law+constant model would be the better description. However, none of our variable AGNs favor this model, likely due to the penalty imposed on the extra parameter. In order to mitigate this bias, in the case where  $P_N$  is comparable to the power spectrum level at high frequencies, we adopt the best-fit power law+constant model over the single power law model. We note that since we are effectively “de-reddening” the power spectrum by first fitting it to a power law and do not aim to measure the “true” PSD slope, we refrain from directly comparing our distribution of the best-fit power law slopes with those measured by [Shimizu & Mushotzky \(2013\)](#), except for noting that, qualitatively, our distribution of slopes would contain more flatter slopes than the [Shimizu & Mushotzky \(2013\)](#) distribution, due to the high level of white noise of the fainter sources in our sample.

#### 2.5. The BAT 105-month sample: Upper limits on periodic signals

After obtaining reasonable fits to the power spectra, we proceed to apply the method in Section 2.2 to test for periodic signals. We have chosen 99.7% as the significance level, since we do not expect any source in our sample to have peaks above this threshold (as a false positive), and we are able to reject the presence of any periodic signal at this level.

The null-detection also allows us to put upper-limit constraints on periodic amplitudes in the BAT volume as a function of frequency. As we show in Figure 4, the most stringent upper limit in log-power units is given by 1ES 0152+022. While the periodogram is conventionally normalized to have fractional rms units, we can also calculate the variability power in terms of “absolute” units and convert to an upper limit in physical units, as the BAT count rate is normalized to the Crab ( $f_{14-195\text{keV}} = 2.33 \times 10^{-8} \text{ erg cm}^{-2} \text{ s}^{-1}$ ). Hence, the best upper limit in physical flux units is provided by NGC 2110, which is also one of the brightest AGNs in the sample (dashed line in Figure 4). We note that those upper limits apply to a strictly periodic signal, rather than a “quasi-periodic” signal, which has a finite width in Fourier frequency.

Given the upper limit of  $\sim 1$  periodic source per  $10^4$  AGNs in optical surveys out to a higher redshift (Liu et al. 2019), a null detection in  $\sim 1000$  BAT AGNs at lower redshifts was to be expected. As we will also show in Section 3.1, the null detection in BAT is consistent with the small amplitudes of binary-induced periodic variability and the large measurement uncertainties of BAT.

### 3. DETECTION PROSPECTS FOR EROSITA

While we do not find periodicities in the BAT sample, the upcoming *eROSITA* mission is likely to transform the search for SMBHBs in the X-rays, thanks to its high sensitivity in the 0.5–10 keV band and its all-sky scanning strategy. In this section, we will attempt to investigate the detectability of SMBHBs as periodic AGNs with *eROSITA*.

More specifically, we will test for periodic signals produced by a mock population of binaries that are superimposed on red noise. Assuming a fixed variance for the red noise PSD (see Section 2.2 and discussions below), only two parameters are needed to generate a light curve — the amplitude and period of the signal. These two elements will then be determined by binary parameters from the mock population. While the *eROSITA* sky is divided by half between the German and Russian consortia, we refer to a full-sky SMBHB population whenever applies.

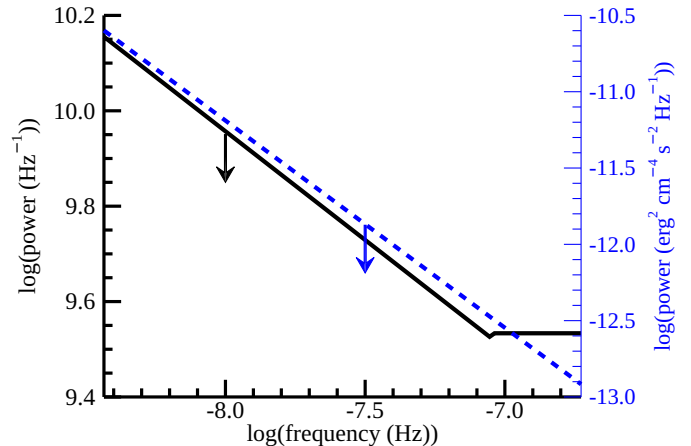


**Figure 4.** The 99% upper limit on a periodic signal determined from the two best sources in the BAT AGN sample, represented here in fractional rms and flux units (black solid and blue dashed lines, respectively). The significance level in the white noise-dominated frequency range is calculated separately and has a different trial factor (i.e. number of frequencies).

#### 3.1. A Mock Periodic AGN Sample

*eROSITA* will be located at the L2 Lagrangian point and scan the sky in great circles, completing one circle in four hours. As its survey plane progresses around the sun by  $\sim 1$  deg per day, *eROSITA* will complete a scan of the full sky every 6 months and eight full-sky scans during its survey lifetime (eRASS:1 – eRASS:8). As a result of this scanning strategy, the ecliptic poles are more frequently visited than lower latitudes and have deeper total exposure (more details can be found in Merloni et al. 2012). Hence, to the contrary of the effectively uniform sky coverage of BAT and the similar observing cadence of a ground-based survey regardless of sky location, searching for periodic AGNs as SMBHB candidates with *eROSITA* faces a unique problem related to the sampling, where there are two possible strategies: (1) visiting a larger number of AGNs at a lower cadence, so that rare variability types of fixed event rates are more likely to be discovered and (2) visiting a smaller number at a higher cadence in order to better sample a wider range of variability timescales (thus possible binary parameters) and better model the normal AGN variability on which a periodic signal may be superimposed.

To investigate this effect, we adopt the mock *eROSITA* AGN catalog of Comparat et al. (2019). The method populates dark matter halos with galaxy stellar masses and then AGNs using an abundance matching technique and reproduces the observed AGN X-ray lumi-

nosity function. For the remainder of the section, we adopt the full mock catalog (“eRASS8”), which includes 2.6 million AGNs at  $0 < z < 6$ . To convert the galaxy stellar mass to the black hole mass, we use the  $M_{\text{stellar}} - M_{\text{BH}}$  relation from Reines & Volonteri (2015)<sup>7</sup>:  $\log(M_{\text{BH}}/M_{\odot}) = 7.45 + 1.05 \log(M_{\text{stellar}}/10^{11}M_{\odot})$ , and the resulting range of  $M_{\text{BH}}$  is  $\sim 10^6 - 10^8 M_{\odot}$  (we will further discuss this scaling relation and our black hole masses below).

We then estimate the number of AGNs near the ecliptic poles given the *eROSITA* scanning strategy. For the purpose of this study, we simply adopt the total exposure time at a given ecliptic latitude  $t_{\text{exp}} \sim 1627 \text{ sec}/\cos(\text{lat})$  and assume  $t_{\text{exp}} = 250 \text{ s}$  per daily visit, so that  $\sim 400 \text{ deg}^2$  of the sky around the poles will be visited at least once per month, and  $\sim 25 \text{ deg}^2$  will be visited at least once per week (“Case A” and “Case B”, respectively). However, it should be noted that this is not the actual sampling of eRASS:1 – eRASS:8. During each 6-month-long full-sky scan, a given sky location will be paid several consecutive visits, which are separated by 6 hours, before *eROSITA* returns to it in the next eRASS. Since the current *eROSITA* scanning strategy is not yet publicly available, we have made a few assumptions about the sampling pattern: (1) we assume the scanning law does not evolve between eRASS:1 – eRASS:8; (2) we have significantly simplified the cadence and adopting a uniform sampling; (3) we have chosen a baseline cadence of once per month which is motivated by the monthly binning of the 105-month BAT light curves. We will discuss the effect of more realistic sampling with gap periods in Section 3.2.

Having determined the sky areas that will be visited at the Case A and B sampling rates, we then select AGNs from the Comparat et al. (2019) catalog that are in those regions using a grid with size  $\Delta\text{RA} = 0.1 \text{ h}$  and  $\Delta\text{dec} = 1 \text{ deg}$  for Case A and a finer grid for Case B:  $\Delta\text{RA} = 0.05 \text{ h}$  and  $\Delta\text{dec} = 0.5 \text{ deg}$ . Hence, Case A and Case B contain  $\sim 8 \times 10^4$  and  $\sim 6 \times 10^3$  AGNs, respectively.

To compute an upper limit on the number of SMBHBs that could exist in this AGN sample, we assume a one-to-one correspondence between an AGN and an SMBHB. This is motivated by the match between the AGN lifetime of  $t_{\text{AGN}} \sim 10^7 \text{ yr}$  and the timescale for a binary to evolve from the outer edge of the circumbinary disk to coalescence (Haiman et al. 2009). We further assume: (1) all binaries in the footprint have evolved into the gravitational wave-emitting regime where the

time (“residence time”) a binary spends at an orbit that corresponds to the orbital timescale  $t_{\text{orb}}$  is  $t_{\text{res}} = 1.11 \times 10^7 \text{ yr } q_s^{-1} M_7^{-5/3} t_{\text{orb}}^{8/3}$  (Haiman et al. 2009), where  $q_s = 4q/(1+q)^2$  with  $q = M_2/M_1$  being the mass ratio,  $M_7 = M_{\text{BH}}/10^7 M_{\odot}$ , and  $t_{\text{orb}}$  is in units of yr; (2) all residence timescales can be probed by either Case A or Case B, i.e.  $t_{\text{res,min}} \sim 10^5 \text{ yr}$  and  $t_{\text{res,max}} \sim 10^7 \text{ yr}$ , and each binary is assigned a residence time according to the linear dependence of the binary number rate on  $t_{\text{res}}$ :  $f(t_{\text{res}}) = t_{\text{res}}/t_{\text{AGN}}$  (Haiman et al. 2009). The upper bound of  $10^7 \text{ yr}$  is motivated by the binary evolution timescale as we previously discussed, above which the binaries can no longer be active as AGNs during their entire lifetimes, and our assumptions are no longer valid. The lower bound is such that the expectation number of binaries with the shortest  $t_{\text{res}}$  is at least a few in a sample of  $10^3 - 10^4$  AGNs. While in principle, the absolute lower limit on  $t_{\text{res}}$  is where the separation  $a = r_{\text{ISCO}}$ , we note that our results should be insensitive to the lower bound on  $t_{\text{res}}$ , since binaries with very short residence timescales are exceedingly rare.

We then “sample” this binary population with *eROSITA* by considering three elements: temporal constraints, flux limit of the survey, and column density of the AGN. Since  $t_{\text{res}} = t_{\text{res}}(t_{\text{orb}}, M_{\text{BH}}, q)$ , we are able to calculate  $t_{\text{orb}}$  and therefore the observed variability timescale of each mock binary:  $t_{\text{var}} = t_{\text{orb}}(1+z)$ . Here we assume  $q = 0.1$ , as it strikes a balance between the mass ratio expected in a major merger and the one that can cause strong periodic modulations (see below). We then only consider those with  $t_{\text{var}}$  that can be probed with the *eROSITA* sampling; thus in Case A,  $t_{\text{var}} = [60, 730] \text{ days}$  and in Case B,  $t_{\text{var}} = [14, 730] \text{ days}$ , assuming at least two cycles are needed for periodicity detection. Second, we impose a soft X-ray band flux limit at  $4.4 \times 10^{-14} \text{ erg s}^{-1} \text{ cm}^{-2}$  (Merloni et al. 2012). Finally, we only consider column densities  $N_{\text{H}} < 10^{23} \text{ cm}^{-2}$ , to which the soft X-ray band is sensitive. A total of 1310 AGNs met this criterion in Case A, and 61 in Case B, and their  $t_{\text{var}}$  distributions are shown in the left panels of Figure 5.

We note a few caveats associated with our binary population: first, the  $M_{\text{stellar}} - M_{\text{BH}}$  relation from Reines & Volonteri (2015) is systematically below that of elliptical galaxies and galaxies with classical bulges, and given the strong mass dependence of the binary residence time, our final mock binary population is also dependent on our particular  $M_{\text{BH}}$  prescription. If an  $M_{\text{stellar}} - M_{\text{BH}}$  relation for ellipticals is adopted instead, so that  $\log(M_{\text{BH}}/M_{\odot}) = 8.95 + 1.04 \log(M_{\text{stellar}}/10^{11}M_{\odot})$  (Reines & Volonteri 2015), the number of observable binaries decreases by

<sup>7</sup> Here we have not considered the possible redshift evolution of the  $M_{\text{stellar}} - M_{\text{BH}}$  relation.

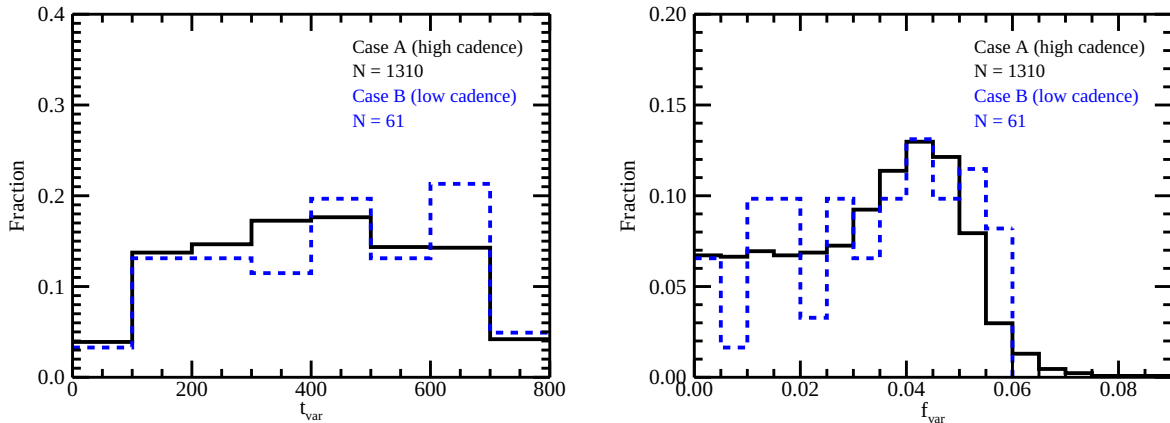


**Figure 5.** Left panel: the variability timescales ( $t_{\text{var}}$ ) of the mock binary population sampled by Case A (black histogram) and Case B (blue dashed histogram). Right panel: their fractional periodic variability amplitudes ( $f_{\text{var}}$ ) under the Doppler model.

a factor of  $\sim 10$ , due to the shorter time for a binary to evolve through the observable timescales. Additionally, since the true  $M_{\text{stellar}} - M_{\text{BH}}$  relation for AGNs is still an active area of inquiry, the aforementioned decrease is likely only a conservative estimate. Second, we have assumed the binary evolution is primarily gravitational wave-driven, so that the residence time has a simple power-law dependence on the orbital period ( $\alpha = 8/3$ ). However, in general,  $\alpha$  is dependent on the physical mechanism driving the binary evolution, and  $\alpha < 8/3$  for other processes such as gas interaction (Haiman et al. 2009). However, those mechanisms are beyond the scope of this work.

To calculate the expected periodic variability amplitude of each AGN, we first consider the relativistic Doppler boost model (D’Orazio et al. 2015). While Doppler boosting is inevitable regardless of the details of the emission, it only gives a conservative estimate of the number of detectable binaries due to its strong dependence on binary parameters and the orbital inclination. In this model, the line-of-sight velocity of the black hole directly translates to an apparent fractional flux variability of its minidisk emission<sup>8</sup>:  $\Delta f/f = (3 - \alpha)(v_2/c) \sin(i)$ , where here we adopt  $\alpha = 1$  as the spectral index in the X-ray band (or a photon index of  $\Gamma = 2$ ),  $v_2$  is the velocity of the secondary black hole:  $v_2 = (2\pi/1 + q)(GM/4\pi^2 P)^{1/3}$ , and we assume random orientations of the binaries on the sky.

In the right panels of Figure 5, we show the resulting distributions of the variability amplitudes. In Case A,

the distribution of  $f_{\text{var}}$  peaks at  $\sim 5\%$  before it sharply declines, so that only 172/1310 or 13% SMBHBs vary at the  $> 5\%$  level. The variability timescales have an essentially flat distribution in the full range of  $t_{\text{var}}$  that can be probed by Case A. However, in Case B, no AGNs at the high  $f_{\text{var}}$  tail are probed, and longer  $t_{\text{var}}$  are more often represented, in contrast with Case A.

We will also consider a second model in the following section, where we assume  $f_{\text{var}} = 10\%$  as an optimistic case. While this variability amplitude is higher than the highest amplitude of the Doppler-boosted periodic binaries in our sample, it may be more consistent with an alternative mechanism that could produce X-ray periodicity due to the outflung gas hitting the cavity wall (see Tang et al. 2018). Unlike Doppler boosting, the periodic amplitude in this model cannot be calculated analytically; thus, we will fix  $f_{\text{var}}$  at 10% for all binary parameters and inclination angles. However, we will adopt the same  $t_{\text{var}}$  distribution, since it is the output of the same binary population.

Working under the same upper-limit assumption that binaries already exist the BAT volume, we also revisited the null detection of periodic AGNs with BAT by adopting the black hole mass and redshift measurements from BASS DR2. While BAT spans a baseline that is at least twice longer (and thus samples a wider range of  $t_{\text{var}}$ ), its measurement uncertainty is much larger than the fractional periodic variability ( $\lesssim 8\%$  level) of any SMBHBs, and a signal can not be detected even without the underlying red noise. This shows that our chosen toy model for the binary population is consistent with the lack of detections in BAT, while they are also able to predict the detectability with eROSITA (Section 3.2).sec:analysis

<sup>8</sup> Here we assume the emission is dominated by the secondary black hole. See Farris et al. (2014) for an accretion prescription of individual members of the binary.

### 3.2. Detectability of Periodic AGNs

To investigate the detectability of a periodic signal of period  $t_{\text{var}}$  and amplitude  $f_{\text{var}}$  superimposed on red noise, we first use the method of [Timmer & Koenig \(1995\)](#) to produce a mock light curve of a given PSD. Here we again adopt a single power law, since the expected PSD break  $T_{\text{br}} \sim \text{day}$  is shorter than the timescales probed by Case A or B, given the black hole masses of the sample (see Section 2.2). We draw the value of the PSD slope  $\alpha$  from a normal distribution of  $\mu = 0.9$  and  $\sigma = 0.2$ , which is consistent with previous studies of the PSD (e.g. [Shimizu & Mushotzky 2013](#)). The normalization  $A$  of the single power law is such that the fractional variability is  $\sim 30\%$ , which is also consistent with our variable AGN sample (Section 2.2 and Figure 1) and largely independent of black hole mass ([Shimizu & Mushotzky 2013](#)).

Next, we inject a periodic signal, so that its period and sinusoidal amplitude are given by  $t_{\text{var}}$  and  $f_{\text{var}}$  of the mock binary, respectively. However, we only consider those with  $f_{\text{var}} > 5\%$  as our minimum signal-to-noise case, where the periodic signal has an amplitude of  $f_{\text{var}}$  as previously defined. We have also added Poisson noise in the light curve: we assume that the measurement uncertainty between visits is negligible compared to the intrinsic stochastic variability; this corresponds to a fractional uncertainty of  $\sim$  a few percent (see Section 2.2). We note that this fraction is likely an underestimate for the fainter sources.

Finally, we down-sample the light curve that is initially daily-sampled on a baseline  $\sim 20$  times longer to the cadence of each mock binary. For the sake of simplicity, we assume that the sampling rate of Case A is exactly once per month, and that of Case B is once per week. In the conservative Doppler model, Case A includes 172 AGNs, and Case B includes 12, and we generated light curves for ten realizations of each case. We show an example from each case in Figure 6. We then repeat the procedure for the optimistic case, where  $f_{\text{var}}$  is fixed at 10%. We do not require a signal-to-noise threshold in this case, and Case A includes 1310 AGNs and Case B includes 61.

We then apply the method in Section 2.2 and search for a periodic signal at the 99% level. The results are summarized in Table 1: in Case A under the conservative model, a few dozens of light curves in each realization are identified as having peaks at this level. We refer to this number as  $N_{\text{cand}}$ , since in a systematic search where a significance level threshold is applied, they would be selected as ‘‘periodic candidates.’’ However, most of them are false positives due to red noise fluctuations, which is indicated by a high-significance peak located at the wrong frequency. Nevertheless, 1–2

binaries ( $\sim 0.5\%$  of the sample) can be identified correctly in 5/10 realizations. Since their injected periods have been recovered at the  $> 99\%$  level, we refer to this number as  $N_{\text{recover}}$ . In the optimistic case, where  $f_{\text{var}}$  is fixed at 10% regardless of the mock binary parameter, the recovered number has significantly increased, where  $\sim 70$  binaries can be identified in each realization, corresponding to a recovery fraction of  $\sim 6\%$ .

While the AGNs in Case B are sampled at a rate four times higher than Case A, the recovered binary number is in fact lower, where only one periodic light curve was recovered in the conservative case. This may be due to the fact that the sample in Case B is ten times smaller and does not sample sufficient number of binaries with large amplitude periodic variations, and therefore it is more challenging to identify them against the same red noise background. This hypothesis can be verified in the optimistic case, where its  $f_{\text{var}}$  is the same as Case A, as well as the power law models for the underlying red noise. The recovery rate has significantly increased, resulting in  $\sim 10$  detected binaries in each realization. The increased recovery fraction is attributed in part to the lower fraction of false positives (represented here by  $1 - \frac{N_{\text{recover}}}{N_{\text{cand}}}$ ) compared to Case A. While modeling the underlying red noise process of an AGN may benefit from denser sampling of its light curve, in a systematic search for SMBHBs whose superimposed periodic amplitudes are unknown *a priori*, observing a large number of AGNs increases the chance of obtaining those with large periodic amplitudes, resulting in a more successful search.

We note that our simple periodogram-based approach is only the preliminary step to *reject* a spurious peak at a low significance level and is not meant to *claim* a periodic signal at a high significance level (see [Vaughan 2005](#)). While the former is easily applicable to a large survey dataset, in order to do the latter, better modeling of the underlying red noise and parameter uncertainties should be fully considered. There exist in the literature many statistical approaches that are more appropriate to test for or determine periods in red noise: [Vaughan \(2010\)](#) and [Angus et al. \(2018\)](#), to name but a few, and hence the success rate may increase if a more optimal method is used.

In fact, standard Fourier methods can no longer be used for the actual sampling of eROSITA, where consecutive visits are followed by observing gaps, the length of which is a function of the latitude of the sky location. When the sampling is uneven and the timescales of interest are comparable to the gap, a maximum likelihood approach to the problem is more appropriate. In the X-ray astronomy literature, maximum likelihood time series

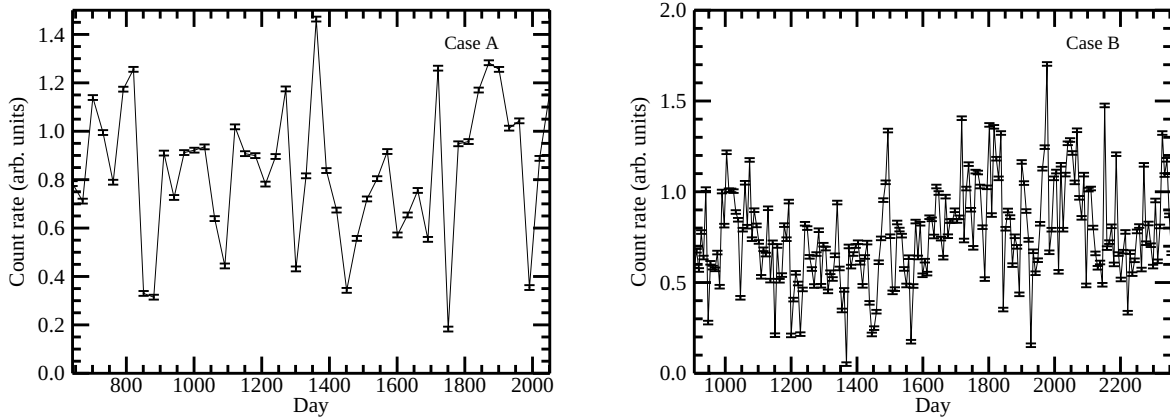


**Figure 6.** Left panel: a simulated light curve in Case A. Right panel: a simulated light curve in Case B.

**Table 1.** Number of recovered periodic AGNs

Case A		Conservative			Optimistic			Case B		Conservative			Optimistic		
Realization	$N_{\text{tot}}$	$N_{\text{cand}}$	$N_{\text{recover}}$	$N_{\text{tot}}$	$N_{\text{cand}}$	$N_{\text{recover}}$	Realization	$N_{\text{tot}}$	$N_{\text{cand}}$	$N_{\text{recover}}$	$N_{\text{tot}}$	$N_{\text{cand}}$	$N_{\text{recover}}$		
1	172	4	0	1310	93	73	1	12	0	0	61	11	9		
2	172	4	0	1310	105	72	2	12	1	0	61	10	9		
3	172	4	0	1310	127	85	3	12	2	1	61	4	4		
4	172	8	1	1310	96	75	4	12	1	0	61	10	10		
5	172	6	1	1310	109	78	5	12	0	0	61	11	10		
6	172	6	0	1310	100	75	6	12	0	0	61	8	7		
7	172	7	0	1310	84	49	7	12	0	0	61	15	13		
8	172	7	1	1310	91	67	8	12	1	0	61	13	10		
9	172	7	2	1310	104	66	9	12	1	0	61	14	12		
10	172	4	1	1310	121	77	10	12	1	0	61	12	9		

analysis methods have been applied to low Earth orbit observations of AGNs by *Suzaku* and *NuSTAR*, for example (e.g. Zoghbi et al. 2013; Kara et al. 2015). In the optical, they have been applied to ground-based time-domain survey datasets, especially those from single-site telescopes where there are large seasonal gaps (e.g. Liu et al. 2018, 2019). Thus, while the Fourier method has the great advantage of speed and can be easily applied to a large (mock) survey dataset, our SMBHB detectability estimates presented here are not meant to replace detailed analyses involving the actual eROSITA sampling.

Finally, we stress that both recovery rates in the “optimistic” and “conservative” cases should be understood as upper limits, since (1) we have assumed that each AGN being sampled hosts an SMBHB, while the actual fraction would be much lower; (2) in both cases, we have assumed that white Poisson noise is negligible with

respect to red noise on the timescales of interest; (3) in our conservative case, we only consider those with large periodic amplitudes, while those with  $f_{\text{var}} < 5\%$  would likely be missed due to red noise, thus further lowering the overall recovery fraction; (4) in our optimistic case, we have fixed the periodic amplitude at 10%; it is therefore “optimistic” in the sense that the periodic amplitude is more pronounced and is independent of binary parameters.

### 3.3. Comparison with Previous Work

The electromagnetic detectability of SMBHBs has been investigated by several previous works. Kelley et al. (2019) used a population of binaries from the Illustris hydrodynamical cosmological simulation and prescribed periodic variability amplitudes based on the hydrodynamical simulations by Farris et al. (2014) or Doppler boost (D’Orazio et al. 2015). They find that a cur-

rent all-sky survey with a magnitude limit of  $\sim 20$  mag is already capable of detecting a few binaries as hydrodynamical periodic AGNs. More encouragingly, they predict that the Large Synoptic Survey Telescope (LSST, Ivezić et al. 2008) can potentially discover more than a hundred periodic AGNs as SMBHBs due to either mechanism, thanks to the much larger volume that it will probe. However, the effect of the underlying red noise has not been explored in that work.

The recent work by Krolik et al. (2019) investigated the detectability of SMBHBs either as a result of a spectral notch in the UV/optical band due to the cavity in the circumbinary disk, or an enhancement in the hard X-rays as the accretion streams shock-heat the minidisks (Roedig et al. 2014). Using a population of binaries similarly “formed” in a cosmological simulation, they predict that there could be  $\sim 100$  binaries with X-ray flux  $> 10^{-13}$  erg s $^{-1}$  cm $^{-2}$  under either model, and X-ray-enhanced binaries are a factor of a few more observable than binaries with the spectral notch feature. While the hard X-ray enhancement should also vary periodically as we discussed in Section 1, identifying such a signature is also susceptible to red noise, since the Compton reflection spectrum in the hard X-ray band should also vary in a stochastic fashion in response to the continuum.

Using an observationally-based approach, Liu et al. (2019) adopted a quasar luminosity function and an empirical variability amplitude–luminosity relation and “selected” variable quasars using the same pipeline as the one applied to their systematic search in the Pan-STARRS1 (Kaiser et al. 2010; Chambers et al. 2016) Medium Deep Survey (PS1 MDS) and converted their upper limit from PS1 MDS to a rate for LSST:  $N_{\text{LSST}} < 3,500$ . Interestingly, if the more conservative expectation value of  $N_{\text{PS1 MDS}} \sim 0.06$  based on the independent predictions by Kelley et al. (2019) is adopted instead, they also arrived at a similar rate of  $N_{\text{LSST}} \sim 200$ .

However, the effect of sampling on the periodicity detection rate was not investigated by any previous work. As we showed in Section 3.2, the high level of red noise and red noise fluctuations hinder the effort to identify periodic signals due to their modest amplitudes, and therefore it is quite possible that of the 100–200 binaries predicted by Kelley et al. (2019) or Krolik et al. (2019), only a fraction can be identified observationally. The exact fraction is strongly dependent on the amplitude of the periodic signal, as we have discussed in Section 3.2.

### 3.4. Remarks on Future Surveys

Assuming an optimistic recovery fraction of 6% and extrapolating the same fraction to the full sky, where

there are  $\sim 2000$  SMBHBs with enhanced hard X-ray emissions at a few tens keV with flux  $f > 10^{-14}$  erg cm $^{-2}$  s $^{-1}$ ,  $\sim 10\%$  of which have short binary periods  $P \lesssim 5$  yr (Krolik et al. 2019), we expect to detect  $\sim 12$  of them with monthly sampling over ten years. This would require an all-sky hard X-ray survey with a sensitivity down to  $10^{-14}$  erg cm $^{-2}$  s $^{-1}$  with a few percent uncertainty; however, the detection of an enhanced hard X-ray emission, accompanied by periodicity, would provide unambiguous evidence for an SMBHB.

## 4. SUMMARY AND CONCLUSIONS

AGNs that host SMBHBs are predicted to vary periodically on roughly the binary orbital timescale from optical to X-rays. We have performed the first systematic search for SMBHBs in the X-rays with *Swift*-BAT. While we do not find evidence for SMBHBs in the first 105 months of BAT data, we investigated the prospects of detecting them with the *eROSITA* survey by constructing an upper-limit rate model for the binary population and taking into account the *eROSITA* scanning strategy, stochastic AGN variability, and periodic variability due to the presence of a binary.

We find that among the simulated binaries that are visited monthly,  $\sim 0.5\%$  can be robustly detected under the Doppler boost model, due to the rarity of large periodic variability amplitudes that can stand out from stochastic AGN variability. In an optimistic model where the periodic variability amplitude is independent of binary parameters,  $\sim 6\%$  of the binaries can be identified. We note, however, that these predictions depend on black hole mass scaling relations and their redshift evolution. Interestingly and more crucially, while one may prefer a higher cadence which allows one to sample a wider range of timescales and better model stochastic AGN variability, on which a periodic signal may be superimposed, a higher cadence does not significantly change the outcome of the search. Therefore, when the total exposure time is fixed, the optimal search strategy for SMBHBs is to maximize the cosmic volume probed by sampling a large number of AGNs, rather than to sample a smaller number at a higher cadence, especially since both merger rate and AGN activity increase with redshift.

TL, MK, and GCP thank the Aspen Center for Physics, which is supported by National Science Foundation grant PHY-1607611, for hosting the “Astrophysics of Massive Black Hole Mergers: From Galaxy Mergers to the Gravitational Wave Regime” workshop, where many stimulating discussions took place and where this work was initiated.

TL is supported by the NANOGrav National Science Foundation Physics Frontiers Center award No. 1430284. MK acknowledges support from NASA through ADAP award NNH16CT03C. LB acknowledges support from National Science Foundation grant AST-1715413. CR acknowledges support from the CONICYT+PAI Convocatoria Nacional subven-

cion a instalacion en la academia convocatoria año 2017 PAI77170080. ET acknowledges support from CONICYT-Chile grants Basal-CATA AFB-170002, FONDECYT Regular 1160999 and 1190818, and Anillo de Ciencia y Tecnología ACT1720033. GCP acknowledges support from the University of Florida.

*Facilities:* Swift(BAT)

## REFERENCES

- Ajello, M., Rebusco, P., Cappelluti, N., et al. 2010, *ApJ*, 725, 1688, doi: [10.1088/0004-637X/725/2/1688](https://doi.org/10.1088/0004-637X/725/2/1688)
- . 2009, *ApJ*, 690, 367, doi: [10.1088/0004-637X/690/1/367](https://doi.org/10.1088/0004-637X/690/1/367)
- Angus, R., Morton, T., Aigrain, S., Foreman-Mackey, D., & Rajpaul, V. 2018, *MNRAS*, 474, 2094, doi: [10.1093/mnras/stx2109](https://doi.org/10.1093/mnras/stx2109)
- Barthelmy, S. D., Barbier, L. M., Cummings, J. R., et al. 2005, *SSRv*, 120, 143, doi: [10.1007/s11214-005-5096-3](https://doi.org/10.1007/s11214-005-5096-3)
- Baumgartner, W. H., Tueller, J., Markwardt, C. B., et al. 2013, *ApJS*, 207, 19, doi: [10.1088/0067-0049/207/2/19](https://doi.org/10.1088/0067-0049/207/2/19)
- Beckmann, V., Barthelmy, S. D., Courvoisier, T. J.-L., et al. 2007, *A&A*, 475, 827, doi: [10.1051/0004-6361/20078355](https://doi.org/10.1051/0004-6361/20078355)
- Begelman, M. C., Blandford, R. D., & Rees, M. J. 1980, *Nature*, 287, 307, doi: [10.1038/287307a0](https://doi.org/10.1038/287307a0)
- Bird, A. J., Bazzano, A., Bassani, L., et al. 2010, *ApJS*, 186, 1, doi: [10.1088/0067-0049/186/1/1](https://doi.org/10.1088/0067-0049/186/1/1)
- Bowen, D. B., Mewes, V., Campanelli, M., et al. 2018, *ApJL*, 853, L17, doi: [10.3847/2041-8213/aaa756](https://doi.org/10.3847/2041-8213/aaa756)
- Bowen, D. B., Mewes, V., Noble, S. C., et al. 2019, *ApJ*, 879, 76, doi: [10.3847/1538-4357/ab2453](https://doi.org/10.3847/1538-4357/ab2453)
- Burke-Spolaor, S., Blecha, L., Bogdanovic, T., et al. 2018, arXiv e-prints. <https://arxiv.org/abs/1808.04368>
- Caballero-Garcia, M. D., Papadakis, I. E., Nicastro, F., & Ajello, M. 2012, *A&A*, 537, A87, doi: [10.1051/0004-6361/201117974](https://doi.org/10.1051/0004-6361/201117974)
- Chambers, K. C., Magnier, E. A., Metcalfe, N., et al. 2016, ArXiv e-prints. <https://arxiv.org/abs/1612.05560>
- Charisi, M., Bartos, I., Haiman, Z., et al. 2016, *MNRAS*, 463, 2145, doi: [10.1093/mnras/stw1838](https://doi.org/10.1093/mnras/stw1838)
- Comparat, J., Merloni, A., Salvato, M., et al. 2019, *MNRAS*, 487, 2005, doi: [10.1093/mnras/stz1390](https://doi.org/10.1093/mnras/stz1390)
- Di Matteo, T., Springel, V., & Hernquist, L. 2005, *Nature*, 433, 604, doi: [10.1038/nature03335](https://doi.org/10.1038/nature03335)
- D’Orazio, D. J., Haiman, Z., & MacFadyen, A. 2013, *MNRAS*, 436, 2997, doi: [10.1093/mnras/stt1787](https://doi.org/10.1093/mnras/stt1787)
- D’Orazio, D. J., Haiman, Z., & Schiminovich, D. 2015, *Nature*, 525, 351, doi: [10.1038/nature15262](https://doi.org/10.1038/nature15262)
- D’Orazio, D. J., & Loeb, A. 2018, *ApJ*, 863, 185, doi: [10.3847/1538-4357/aad413](https://doi.org/10.3847/1538-4357/aad413)
- Edelson, R., Turner, T. J., Pounds, K., et al. 2002, *ApJ*, 568, 610, doi: [10.1086/323779](https://doi.org/10.1086/323779)
- Farris, B. D., Duffell, P., MacFadyen, A. I., & Haiman, Z. 2014, *ApJ*, 783, 134, doi: [10.1088/0004-637X/783/2/134](https://doi.org/10.1088/0004-637X/783/2/134)
- . 2015, *MNRAS*, 446, L36, doi: [10.1093/mnrasl/slu160](https://doi.org/10.1093/mnrasl/slu160)
- Gehrels, N., Chincarini, G., Giommi, P., et al. 2004, *ApJ*, 611, 1005, doi: [10.1086/422091](https://doi.org/10.1086/422091)
- Gold, R., Paschalidis, V., Etienne, Z. B., Shapiro, S. L., & Pfeiffer, H. P. 2014, *PhRvD*, 89, 064060, doi: [10.1103/PhysRevD.89.064060](https://doi.org/10.1103/PhysRevD.89.064060)
- González-Martín, O., & Vaughan, S. 2012, *A&A*, 544, A80, doi: [10.1051/0004-6361/201219008](https://doi.org/10.1051/0004-6361/201219008)
- Graham, M. J., Djorgovski, S. G., Stern, D., et al. 2015a, *Nature*, 518, 74, doi: [10.1038/nature14143](https://doi.org/10.1038/nature14143)
- . 2015b, *MNRAS*, 453, 1562, doi: [10.1093/mnras/stv1726](https://doi.org/10.1093/mnras/stv1726)
- Haiman, Z. 2017, *PhRvD*, 96, 023004, doi: [10.1103/PhysRevD.96.023004](https://doi.org/10.1103/PhysRevD.96.023004)
- Haiman, Z., Kocsis, B., & Menou, K. 2009, *ApJ*, 700, 1952, doi: [10.1088/0004-637X/700/2/1952](https://doi.org/10.1088/0004-637X/700/2/1952)
- Harrison, F. A., Craig, W. W., Christensen, F. E., et al. 2013, *ApJ*, 770, 103, doi: [10.1088/0004-637X/770/2/103](https://doi.org/10.1088/0004-637X/770/2/103)
- Hopkins, P. F., Hernquist, L., Cox, T. J., & Kereš, D. 2008, *ApJS*, 175, 356, doi: [10.1086/524362](https://doi.org/10.1086/524362)
- Ivezic, Z., Tyson, J. A., Abel, B., et al. 2008, ArXiv e-prints. <https://arxiv.org/abs/0805.2366>
- Kaiser, N., Burgett, W., Chambers, K., et al. 2010, in Society of Photo-Optical Instrumentation Engineers (SPIE) Conference Series, Vol. 7733, Society of Photo-Optical Instrumentation Engineers (SPIE) Conference Series, 0
- Kara, E., Zoghbi, A., Marinucci, A., et al. 2015, *MNRAS*, 446, 737, doi: [10.1093/mnras/stu2136](https://doi.org/10.1093/mnras/stu2136)
- Kelley, L. Z., Haiman, Z., Sesana, A., & Hernquist, L. 2019, *MNRAS*, 485, 1579, doi: [10.1093/mnras/stz150](https://doi.org/10.1093/mnras/stz150)
- Kollmeier, J. A., Zasowski, G., Rix, H.-W., et al. 2017, ArXiv e-prints. <https://arxiv.org/abs/1711.03234>

- Koss, M., Mushotzky, R., Treister, E., et al. 2012, *ApJL*, 746, L22, doi: [10.1088/2041-8205/746/2/L22](https://doi.org/10.1088/2041-8205/746/2/L22)
- Koss, M., Trakhtenbrot, B., Ricci, C., et al. 2017, *ApJ*, 850, 74, doi: [10.3847/1538-4357/aa8ec9](https://doi.org/10.3847/1538-4357/aa8ec9)
- Koss, M. J., Assef, R., Baloković, M., et al. 2016, *ApJ*, 825, 85, doi: [10.3847/0004-637X/825/2/85](https://doi.org/10.3847/0004-637X/825/2/85)
- Koss, M. J., Blecha, L., Bernhard, P., et al. 2018, *Nature*, 563, 214, doi: [10.1038/s41586-018-0652-7](https://doi.org/10.1038/s41586-018-0652-7)
- Krivonos, R., Tsygankov, S., Revnivtsev, M., et al. 2010, *A&A*, 523, A61, doi: [10.1051/0004-6361/201014935](https://doi.org/10.1051/0004-6361/201014935)
- Krolik, J. H., Volonteri, M., Dubois, Y., & Devriendt, J. 2019, *ApJ*, 879, 110, doi: [10.3847/1538-4357/ab24c9](https://doi.org/10.3847/1538-4357/ab24c9)
- Liu, T., Gezari, S., & Miller, M. C. 2018, *ApJL*, 859, L12, doi: [10.3847/2041-8213/aac2ed](https://doi.org/10.3847/2041-8213/aac2ed)
- Liu, T., Gezari, S., Heinis, S., et al. 2015, *ApJL*, 803, L16, doi: [10.1088/2041-8205/803/2/L16](https://doi.org/10.1088/2041-8205/803/2/L16)
- Liu, T., Gezari, S., Burgett, W., et al. 2016, *ApJ*, 833, 6, doi: [10.3847/0004-637X/833/1/6](https://doi.org/10.3847/0004-637X/833/1/6)
- Liu, T., Gezari, S., Ayers, M., et al. 2019, *ApJ*, 884, 36, doi: [10.3847/1538-4357/ab40cb](https://doi.org/10.3847/1538-4357/ab40cb)
- MacFadyen, A. I., & Milosavljević, M. 2008, *ApJ*, 672, 83, doi: [10.1086/523869](https://doi.org/10.1086/523869)
- Markwardt, C. B., Tueller, J., Skinner, G. K., et al. 2005, *ApJL*, 633, L77, doi: [10.1086/498569](https://doi.org/10.1086/498569)
- McHardy, I. M., Koerding, E., Knigge, C., Uttley, P., & Fender, R. P. 2006, *Nature*, 444, 730, doi: [10.1038/nature05389](https://doi.org/10.1038/nature05389)
- Merloni, A., Predehl, P., Becker, W., et al. 2012, arXiv e-prints. <https://arxiv.org/abs/1209.3114>
- Merloni, A., Alexander, D. A., Banerji, M., et al. 2019, arXiv e-prints. <https://arxiv.org/abs/1903.02472>
- Nandra, K., George, I. M., Mushotzky, R. F., Turner, T. J., & Yaqoob, T. 1997, *ApJ*, 476, 70, doi: [10.1086/303600](https://doi.org/10.1086/303600)
- Noble, S. C., Mundim, B. C., Nakano, H., et al. 2012, *ApJ*, 755, 51, doi: [10.1088/0004-637X/755/1/51](https://doi.org/10.1088/0004-637X/755/1/51)
- Oh, K., Koss, M., Markwardt, C. B., et al. 2018, *ApJS*, 235, 4, doi: [10.3847/1538-4365/aaa7fd](https://doi.org/10.3847/1538-4365/aaa7fd)
- Papadakis, I. E., & Lawrence, A. 1993, *MNRAS*, 261, 612, doi: [10.1093/mnras/261.3.612](https://doi.org/10.1093/mnras/261.3.612)
- Reines, A. E., & Volonteri, M. 2015, *ApJ*, 813, 82, doi: [10.1088/0004-637X/813/2/82](https://doi.org/10.1088/0004-637X/813/2/82)
- Ricci, C., Ueda, Y., Koss, M. J., et al. 2015, *ApJL*, 815, L13, doi: [10.1088/2041-8205/815/1/L13](https://doi.org/10.1088/2041-8205/815/1/L13)
- Ricci, C., Bauer, F. E., Treister, E., et al. 2017a, *MNRAS*, 468, 1273, doi: [10.1093/mnras/stx173](https://doi.org/10.1093/mnras/stx173)
- Ricci, C., Trakhtenbrot, B., Koss, M. J., et al. 2017b, *ApJS*, 233, 17, doi: [10.3847/1538-4365/aa96ad](https://doi.org/10.3847/1538-4365/aa96ad)
- Rodriguez, C., Taylor, G. B., Zavala, R. T., et al. 2006, *ApJ*, 646, 49, doi: [10.1086/504825](https://doi.org/10.1086/504825)
- Roedig, C., Krolik, J. H., & Miller, M. C. 2014, *ApJ*, 785, 115, doi: [10.1088/0004-637X/785/2/115](https://doi.org/10.1088/0004-637X/785/2/115)
- Satyapal, S., Secrest, N. J., Ricci, C., et al. 2017, *ApJ*, 848, 126, doi: [10.3847/1538-4357/aa88ca](https://doi.org/10.3847/1538-4357/aa88ca)
- Segreto, A., Cusumano, G., Ferrigno, C., et al. 2010, *A&A*, 510, A47, doi: [10.1051/0004-6361/200911779](https://doi.org/10.1051/0004-6361/200911779)
- Severgnini, P., Cicone, C., Della Ceca, R., et al. 2018, *MNRAS*, 479, 3804, doi: [10.1093/mnras/sty1699](https://doi.org/10.1093/mnras/sty1699)
- Shi, J.-M., & Krolik, J. H. 2016, *ApJ*, 832, 22, doi: [10.3847/0004-637X/832/1/22](https://doi.org/10.3847/0004-637X/832/1/22)
- Shi, J.-M., Krolik, J. H., Lubow, S. H., & Hawley, J. F. 2012, *ApJ*, 749, 118, doi: [10.1088/0004-637X/749/2/118](https://doi.org/10.1088/0004-637X/749/2/118)
- Shimizu, T. T., & Mushotzky, R. F. 2013, *ApJ*, 770, 60, doi: [10.1088/0004-637X/770/1/60](https://doi.org/10.1088/0004-637X/770/1/60)
- Soldi, S., Beckmann, V., Baumgartner, W. H., et al. 2014, *A&A*, 563, A57, doi: [10.1051/0004-6361/201322653](https://doi.org/10.1051/0004-6361/201322653)
- Tang, Y., Haiman, Z., & MacFadyen, A. 2018, *MNRAS*, 476, 2249, doi: [10.1093/mnras/sty423](https://doi.org/10.1093/mnras/sty423)
- Timmer, J., & Koenig, M. 1995, *A&A*, 300, 707
- Tueller, J., Mushotzky, R. F., Barthelmy, S., et al. 2008, *ApJ*, 681, 113, doi: [10.1086/588458](https://doi.org/10.1086/588458)
- Tueller, J., Baumgartner, W. H., Markwardt, C. B., et al. 2010, *ApJS*, 186, 378, doi: [10.1088/0067-0049/186/2/378](https://doi.org/10.1088/0067-0049/186/2/378)
- Ubertini, P., Lebrun, F., Di Cocco, G., et al. 2003, *A&A*, 411, L131, doi: [10.1051/0004-6361:20031224](https://doi.org/10.1051/0004-6361:20031224)
- Vaughan, S. 2005, *A&A*, 431, 391, doi: [10.1051/0004-6361:20041453](https://doi.org/10.1051/0004-6361:20041453)
- . 2010, *MNRAS*, 402, 307, doi: [10.1111/j.1365-2966.2009.15868.x](https://doi.org/10.1111/j.1365-2966.2009.15868.x)
- Vaughan, S., Edelson, R., Warwick, R. S., & Uttley, P. 2003, *MNRAS*, 345, 1271, doi: [10.1046/j.1365-2966.2003.07042.x](https://doi.org/10.1046/j.1365-2966.2003.07042.x)
- Wik, D. R., Sarazin, C. L., Finoguenov, A., et al. 2011, *ApJ*, 727, 119, doi: [10.1088/0004-637X/727/2/119](https://doi.org/10.1088/0004-637X/727/2/119)
- Winkler, C., Courvoisier, T. J.-L., Di Cocco, G., et al. 2003, *A&A*, 411, L1, doi: [10.1051/0004-6361:20031288](https://doi.org/10.1051/0004-6361:20031288)
- Zoghbi, A., Reynolds, C., & Cackett, E. M. 2013, *ApJ*, 777, 24, doi: [10.1088/0004-637X/777/1/24](https://doi.org/10.1088/0004-637X/777/1/24)